Novel Crankshaft Mechanism and Regenerative Braking System to Improve the Fuel Economy of Passenger Cars

Alberto Boretti and Joseph Scalzo

Abstract Improvements of vehicle fuel economy may be achieved by the introduction of advanced internal combustion engines (ICE) improving the fuel conversion efficiency of the engine and of advanced power trains (PWT) reducing the amount of fuel energy needed to power the vehicle. The paper presents a novel design of a variable compression ratio advanced spark ignition engine that also permits an expansion ratio that may differ from the compression ratio hence generating an Atkinson cycle effect. The stroke ratio and the ratio of maximum to minimum in-cylinder volumes may change with load and speed to provide the best fuel conversion efficiency. The variable ratio of maximum to minimum in-cylinder volumes also improves the full load torque output of the engine. The paper also presents an evolved mechanical kinetic energy recovery system delivering better round trip efficiencies with a design tailored to store a smaller quantity of energy over a reduced time frame with a non-driveline configuration. Simulations show an improvement of full load torque output and fuel conversion efficiency. Brake specific fuel consumption maps are computed for a gasoline engine 2 litres, in-line four, turbocharged and directly fuel injected showings significant fuel savings during light and medium loads operation. Results of vehicle driving cycle simulations are presented for a full size car equipped with the 2 L turbo GDI engine and a compact car with a downsized 1 L turbo GDI engine. These results show dramatic improvements of fuel economies for

F2012-A01-004

A. Boretti (✉)
Missouri University of Science and Technology, Rolla, MO, USA
e-mail: a_boretti@yahoo.com

A. Boretti
University of Ballarat, Ballarat, VIC, Australia

J. Scalzo
Scalzo Automotive Research Pty Ltd, Melbourne, VIC, Australia

SAE-China and FISITA (eds.), *Proceedings of the FISITA 2012 World Automotive Congress*, Lecture Notes in Electrical Engineering 189,
DOI: 10.1007/978-3-642-33841-0_2,

similar to Diesel fuel energy usage and CO_2 production. The turbo GDI engines with the alternative crank trains offer better than hybrids fuel economies if the vehicles are also equipped with the novel mechanical kinetic energy recovery system (KERS) recovering the braking energy to reduce the thermal energy supply in the following acceleration of a driving cycle.

Keywords Fuel economy · Carbon dioxide emissions · Environmentally friendly transport · Alternative crank train mechanisms · Variable compression ratio · Atkinson cycle · Mechanical kinetic energy recovery systems

1 Introduction

Direct fuel injection (DI), turbo charging (TC) and downsizing are the major features in stoichiometric gasoline engines currently being adopted to dramatically improve the fuel economy during driving cycles and therefore largely reduce the emissions of carbon dioxide. With these features, stoichiometric gasoline engines still have lower top and part load fuel efficiencies versus higher compression ratio, lean burning Diesel engines being controlled throttle-less by quantity of fuel injected, but have the advantage of much higher power densities for a better downsizing. Furthermore, stoichiometric gasoline engines have very low air pollutant emissions thanks to the well established three-way catalyst technology to meet future emission regulations much easier than Diesel [1, 2]. Major areas of development are variable valve actuation (VVA), exhaust gas recirculation (EGR), variable compression ratio (VCR), and alternative power cycles as well as crank train mechanisms all to boost the fuel conversion efficiency. Aim of this paper is to present a new crank train mechanism enabling variable compression ratio and variable Atkinson effect applied to one of the latest turbo GDI engine.

The Atkinson cycle engine is basically an engine permitting the strokes to be of different lengths. In the Atkinson cycle, the power and exhaust strokes are longer than the intake and compression strokes and should result in better fuel efficiency. Atkinson designed more than one engine to capitalize on this important property. The original Atkinson cycle engine allowed the intake, compression, power, and exhaust strokes of the four-stroke cycle to occur in a single turn of the crankshaft and was designed to avoid infringing patents covering Otto cycle engines. Because of the unique crankshaft design of the Atkinson engine, its expansion stroke can differ from its compression stroke and, with a power stroke longer than its compression stroke the engine can achieve larger thermal efficiency than a traditional engine. The disadvantage of the four-stroke Atkinson cycle engine versus the more common Otto cycle engine is reduced power density. Because a smaller portion of the compression stroke is devoted to compressing the intake charge, an Atkinson cycle engine does not take in as much charge as a similar Otto cycle engine would do. Although the Atkinson's original design is merely a historical curiosity, many

modern engines use unconventional valve timing to produce the effect of a shorter compression stroke/longer power stroke, but a few solutions have also been proposed with a different means of linking the piston to the crankshaft [3–10].

Variable compression ratio is the technology to adjust internal combustion engine cylinder compression ratios to increase fuel efficiency under varying loads [11–25]. Higher loads require lower ratios to be more efficient and vice versa. Variable compression engines allow for the volume above the piston at top dead centre to be changed. For automotive use this needs to be done dynamically in response to the load and driving demands. Output of spark ignition engines is controlled by the quantity of mixture introduced within the cylinder. Occurrence of knock limits the values of compression ratio and boost pressures that can be adopted in turbocharged spark ignition engines or the compression ratio that may be used in naturally aspirated spark ignition engines. If the compression ratio is set to avoid knock in the most unsafe wide open throttle operating points, then especially under light loading, the engine can lack torque. The solution is to be able to vary the compression ratio to suit the reduced amount of charge introduced within the cylinder. In all the variable compression ratio systems, the basic advantage is the one that may follow the increased indicated efficiency of the cycle actually not that much in absolute values (increasing the compression ratio the efficiency increase but the theoretical curve has an asymptotic limit). But obviously small changes in absolute values of efficiency may produce large percentage increases in fuel economy especially at very low loads. Coupling of variable compression ratio to turbo charging may increase the options to achieve better fuel economies through synergies with downsizing and pressure boost.

In the present approach, a new mechanism is defined to change not only the compression ratio but also the length of intake, compression, expansion and exhaust strokes as in Atkinson cycles. This system is employed to improve the light load efficiency as well as to boost the full load output and efficiency seeking operation in every point with same margins to knock and switching to expansion strokes longer than compression strokes when more efficient at light loads. The system is fitted on an in-line four cylinder turbocharged gasoline engine with direct fuel injection.

The idea of using a link of the piston to the crankshaft enabling both variable compression ratio and variable ratio of the expansion to the compression stroke is a novelty, as well as a novelty is the opportunity to use the technique to improve the fuel economy over the full range of loads and speed and boost the power output. Because the efficiency increase are limited (or the efficiency actually starts to reduce) increasing the compression ratio over a certain value, we consider here a maximum CR of 15.5:1 and a minimum CR of 9.5:1. The combustion chamber shape is optimized for the 15.5:1 CR, and the lower CR of 9.5:1 is obtained by increasing the piston to head clearances. The lowest CR operating conditions therefore may suffer from poor combustion chamber shape in addition to the penalty due to the reduced combustion pressure and temperature on the evolution of combustion. With regards to the Atkinson cycle effect, the lengths of the expansion, exhaust, intake and compression strokes differ. The TDC piston positions at the start of the expansion and the intake strokes, as well as the BDC

positions at the start of the exhaust and compression strokes also differ. The in-cylinder volumes in the two TDC and in the two BDC are therefore also different. The CR ratio when the Atkinson cycle is enabled refers to the ratio in between the maximum in-cylinder volume at the end of the expansion stroke and the minimum in-cylinder volume at the beginning of the expansion stroke. We consider here an exhaust to intake stroke ratio 1 (no Atkinson) to 1.05. Because of the variability of the stroke, the two TDC and the two BDC volumes differ. Therefore, CR with Atkinson is conventionally defined as the ratio of maximum to minimum in-cylinder volume over the two strokes.

Regenerative braking is finally considered to reduce the thermal engine energy supply when covering driving cycles characterized by accelerations following decelerations, where part of the propulsive power needed to accelerate the car may be the braking energy recovered with a regenerative device. Mechanical regenerative systems are much more efficient than electric regenerative systems permitting almost double the round trip efficiency wheels to wheels [26–32]. While first generation mechanical kinetic energy recovery systems (KERS) were delivering round trip efficiencies of 70 %, today's second generation mechanical KERS are designed to derive round trip efficiencies of almost 80 % thanks to the better attention to the power and energy storage capacity and times of passenger car applications and the focus on improving the efficiency of the constant variable transmission that was the weak part of the first generation KERS design as well as on the off driveline configuration.

2 Mechanism for Variable Compression and Stroke Ratios

The mechanism is comprised of a four bar mechanism that connects the piston to the crankshaft via an oscillating member, positioned on the opposite side of the cylinder relative to the crankshaft. The oscillating member is supported on an eccentric shaft that rotates at half shaft speed preferably in the same direction as the crankshaft, and driven by the crankshaft. A phasing mechanism between the crankshaft and the eccentric shaft allows relative angular motion between the two shafts. This relative motion allows the compression ratio to be altered continuously between two set limits. The size of the eccentric and angular movement of the control shaft determines the extent of the CR adjustment. The maximum angular phasing is approximately 50° and is determined by the control shaft eccentric offset generally not more than 5 mm.

Another feature of the mechanism is that it has an inherent Atkinson cycle phase as well as an exhaust gas retention phase, at various settings of the CR adjustment. Figure 1 shows the piston in the low and high CR positions at TDC and BDC positions. For a typical small engine in this position, when the engine is at a wider throttle open condition and under heavier loads, the induction stroke may be a little shorter than the compression stroke (by about 2 %) and this may produce a small supercharging effect. In addition, the induction stroke is shorter

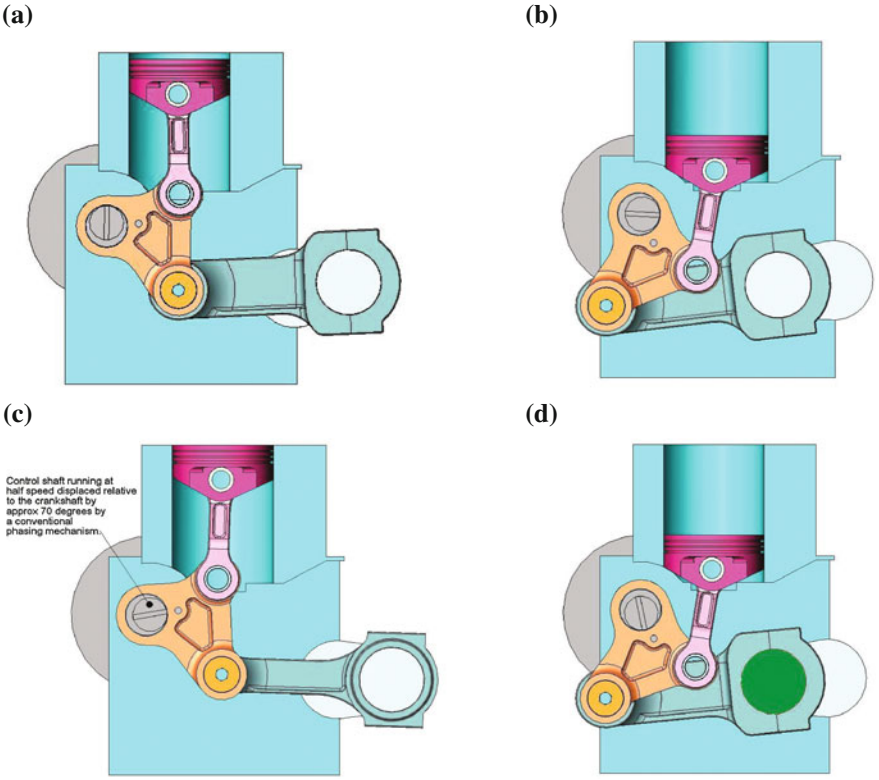

Fig. 1 Low and high CR mechanism at TDC (**a**, **c**) and BDC (**b**, **d**)

than the power stroke and this may produce an Atkinson effect (by about 11 %). Also there is no exhaust gas retention. In the high CR position, when the engine is at lower throttle settings and under lower loads, the induction stroke may be shorter than the compression stroke (by about 6 %) and this may produces a reasonable supercharging effect as well as the Atkinson effect (by about 11 %). Also there is a small gas retention feature. The mechanism can be configured in all in-line engines and all V type engines by having a control shaft for each bank of cylinders in a back to back arrangement with a common crankshaft. By varying the extent of the eccentric and the geometric position of the eccentric shaft, a number of different characteristics can be achieved. For example, an Atkinson effect can be achieved in both low and high CR of up to 20 and 10 % respectively.

It is to be noted that all connections are pin jointed and use known conventional technologies and production techniques. The use of a forked piston con-rod allows the main con-rod to be received in the cavity. Initial dynamic simulation studies indicate that the inertia and combustion loads on the various connections are within the bearing pressure limits of conventional bearing materials. It has also

shown that the engine can be balanced to acceptable levels without the need of balance shafts.

The baseline engine the VCR and Atkinson engine is derived from has a compression ratio CR of 9.5:1. This is the value considered as the lower limit in the Variable Compression Ratio mechanism. For the upper limit, the CR of 15.5:1 is selected to provide the best trade-off for performance and complexity of the mechanism. Increasing the compression ratio, the engine brake thermal efficiency increases. However, after a certain value of the compression ratio, these increments became smaller and smaller, and any further increases of the compression ratio does not warrant the increased structural implications.

The occurrence of knock also limits the maximum compression ratio the engine can use. When using higher compression ratios the turbocharger boosting should be reduced to avoid knock by-passing the turbocharger through the waste gate open. Finally, the complexity of the mechanism increases requiring larger variations, and this may brings additional frictional losses. This value CR = 15.5 follows a preliminary consideration of all these factors. A better analysis may very likely suggest different upper as well as lower boundaries. The use of a variable compression ratio permits to operate the engine close to a preselected margin to the occurrence of knock. The compression ratio became another parameter to be optimized over the speed and load range as it is for the waste gate opening and the spark timing to deliver knock-free the best engine brake thermal efficiency or maximize the torque and power output.

Combustion chambers designed for a CR of 9.5:1 usually do not need too much of squish areas or crowned pistons. Therefore, if the combustion chamber is designed in the variable compression ratio engine for a CR of 15.5:1, when the reduced compression ratio is obtained by increasing the Top Dead Centre (TDC) piston-to-head clearance, we can expect to move from a combustion chamber better than the 9.5:1 fixed compression ratio one to another similar to the 9.5:1 fixed compression ratio one. We do not expect therefore higher engine out emissions especially higher unburned hydrocarbon emissions when lower compression ratio are used in the variable compression ratio mechanism. The combustion chamber shape may be optimized for the higher CR of 15.5:1, with the lower CR of 9.5:1 being obtained by increasing the piston to head clearances. The lowest CR operating conditions therefore may suffer from the only relatively poorer combustion chamber shape in addition to the penalty due to the reduced combustion pressure and temperature on the evolution of combustion. The mechanism permits to change freely the compression ratio in between the minimum and maximum values. The response to changes in compression ratio is similar to the response to the variable valve timing mechanism in modern engines, however this is a subject that needs to be further investigated. The virtual elimination of piston side thrust due to the small piston conrod angular movement will reduce piston friction and may well compensate for any friction caused by the additional pin connections. This will also need to be further investigated.

With reference to the Atkinson cycle effect, the lengths of the expansion, exhaust, intake and compression strokes differ. The TDC piston positions at the

start of the expansion and the intake strokes, as well as the BDC positions at the start of the exhaust and compression strokes also differ. The in-cylinder volumes in the two TDC and in the two BDC are therefore also different. The CR ratio when the Atkinson cycle is enabled refers to the ratio in between the maximum in-cylinder volume at the end of the expansion stroke and the minimum in-cylinder volume at the beginning of the expansion stroke. We consider here an exhaust to intake stroke ratio 1 (no Atkinson) to 1.05. Because of the variability of the stroke, the two TDC and the two BDC volumes differ. Therefore, CR with Atkinson is conventionally defined as the ratio of maximum to minimum in-cylinder volume over the two strokes.

The major areas of concern of the mechanism are costs, complexity, reliability, effectiveness steady state and transient, packaging. It is obvious that the mechanism is more complex than the conventional piston-conrod-crank arrangement, however all of the connections use pressure lubricated conventional pin joints and the eccentric shaft is hydro-dynamically lubricated. The reliability should not be any different than a conventional engine given that the bearing pressures can be designed to be within the limits of conventional bearing materials, taking into consideration, the higher inertia loads produced by the mechanism. This will also have a limitation on the maximum engine speed, however engines adopting this approach, are designed for economy rather than very high speed. For the larger engines the speed factor is generally not an issue as the mechanism can be designed to operate effectively up to 5000 rpm. In comparison with other known mechanisms used for VCR, this mechanism offers simplicity and compactness. The additional components will also add costs and weight. The components are simple to manufacture in mass production and should not add more than 5 % to the cost of the overall engine, and similarly to the overall weight. This additional cost is small compared to the fuel savings and can be recouped in a very short time by the customer. For in-line engines, the packaging is similar to a conventional engine except for a small crankshaft offset that can be a benefit to front drive vehicles. For V type engines the packaging is very similar to a conventional engine and should not create any difficulties. It is to be noted that patent protection has been applied for the nominated mechanism in all the major vehicle producing countries.

While the variable compression ratio is absolutely not a novelty, the way to achieve this variability and the control of this feature linked to a knock sensor to operate all over the range of engine speeds and loads as close as possible to about same margin to knock is certainly an interesting new option offered by this paper.

3 Engine Results for a 2 Litres Turbo GDI

Engine performance simulations have been performed with the GT-SUITE code [33] for a 2 Litres in-line four cylinder turbo charged gasoline engine. The engine geometry (baseline) is presented in Table 1. For the evaluation of benefits of the alternative crank train mechanisms proposed here, there is no reason to modify the

Table 1 2 L in-line four gasoline engine geometry

Displacement per cylinder (L)	0.4995	Number of intake valve per cylinder	2
Number of cylinders	4	Intake valve diameter (mm)	34.5
Engine layout	L-4	Intake valve maximum lift (mm)	10.05
Compression ratio	10	IVO (deg)	358 (−2)
Bore (mm)	86	IVC (deg)	619 (+79)
Stroke (mm)	86	No. of exhaust valve per cylinder	2
Connecting rod length (mm)	143	Exhaust valve dia. (mm)	31
Wrist pin offset (mm)	0	Exhaust valve maximum lift (mm)	10
Clearance volume (L)	0.0550	EVO (deg)	131 (−49)
Engine type	S.I.	EVC (deg)	384 (+24)

design of the intake to follow the variable compression ratio or the variable compression ratio and stroke ratio. Further refinements of the design of the engine with alternative crank train mechanisms are certainly possible in both the intake and the exhaust systems including pipe lengths and diameters as well as valve lift profiles. These refinements may certainly further improve the brake fuel conversion efficiency as well as the torque output.

A modified form of the Chen–Flynn correlation is used to model friction [33, 34]. The correlation has a constant term (for accessory friction), a term which varies with peak cylinder pressure, a third term linearly dependent on mean piston velocity (for hydrodynamic friction) and a fourth term quadratic with mean piston velocity (for windage losses). Values used for the operation with all the cylinders are presented in Table 2. A_{cf} is the constant portion of the Chen–Flynn friction correlation, B_{cf} the term which varies linearly with peak cylinder pressure, C_{cf} the term accounting for hydrodynamic friction in the power cylinder which varies linearly with the piston speed and Q_{cf} the term which varies quadratically with the piston speed and accounts for windage losses in the power cylinder. The equation used to calculate friction is given below:

$$FMEP = A_{cf} + \frac{1}{ncyl}\sum_{i=1}^{ncyl}\left[B_{cf}\cdot(P_{cyl})_i + C_{cf}\cdot(S_{fact})_i + Q_{cf}\cdot(S_{fact})_i^2\right] \quad (1)$$

with: $S_{fact} = ½{\cdot}RPM{\cdot}S$, $A_{cf,}$ $B_{cf,}$ C_{cf} and Q_{cf} user inputs, P_{max} the maximum cylinder pressure, RPM the cycle-average engine speed and S the cylinder stroke. Each cylinder has its own contribution to the total engine friction based upon its own maximum cylinder pressure and stroke (folded into the speed factor, S_{fact}).

The proposed parameters for the FMEP correlations are those following fit of experimental data from measured BMEP and IMEP (output of torque meter and pressure cycles recorded through an in-cylinder pressure sensor) of the GDI turbo engine with a traditional crank train. Despite the new crank train it is not expected to have FMEP values differing too much from those defined above, the subject obviously need further investigation, with assembly of an engine now planned for future tests. Only these experiments may provide a better estimation of the FMEP

Table 2 2 L in-line four gasoline engine friction correlation parameters

Engine operation	L-4
A_{cf} (bar)	0.3
B_{cf}	0.006
C_{cf} (bar s/m)	0.09
Q_{cf} (bar s^2/m^2)	0

versus speed and load of the new engine with a novel crank train mechanism never tested before.

Combustion is modeled using a non-predictive Wiebe combustion model [33] with the look up table from the baseline configuration modified by using the predictive Spark Ignition turbulent combustion model [33] simulations. Simulations were performed with either (1) a non-predictive Wiebe function combustion model [33] with angles for 50 % mass fuel burned and angles for 10–90 % combustion tabled versus engine speed and BMEP from data measured for a GDI turbo engine and a traditional crank train, and (2) a predictive Spark Ignition turbulent combustion model [33] calibrated to reproduce these same experimental data. These two models are very well known models adopted in engine performance simulations over several decades with details eventually available in [33]. This latter predictive model properly calibrated was then used to evaluate the combustion performances with variable spark timing for all the engine solutions considered with the novel crank trains. Knock limited maximum brake torque spark timings were obtained performing simulations for different values of the spark advance and monitoring torque and knock index to select the best spark advance within the constraints. It is worth mentioning that in consideration of the fact the predictive spark ignition turbulent combustion model may fail in some points of a full engine map, we decided to run the final simulations with a non-predictive Wiebe function combustion model [33] having angles for 50 % mass fuel burned and angles for 10–90 % combustion tabled versus engine speed and BMEP from data measured for the GDI turbo engine and a traditional crank train corrected for the results of the predictive spark ignition turbulent combustion model for the actual engine crank trains simulated.

The simple knock model is based on the Douaud and Eyzat induction time correlation [33, 35]. The induction time (ignition delay) in seconds is calculated at every time step using the equation:

$$\tau = \frac{0.01869}{A_p} \cdot \left(\frac{ON}{100}\right)^{3.4107} \cdot P^{-1.7} \cdot \exp\left(\frac{3800}{A_T \cdot T}\right) \tag{2}$$

where A_p is a user-entered pre-exponential multiplier, ON the user-entered fuel octane number (RON 95 in the particular application to gasoline), P the cylinder pressure (kg_f/cm^2), A_T the user-entered activation temperature multiplier and T the unburned gas temperature (K). In general, this induction time continually decreases as combustion progresses and the unburned zone temperature rises. The

end-gas auto-ignites (knocks) if the induction time is less than the flame arrival time. The model assumes that auto-ignition occurs when:

$$\int_{t0}^{ti} \frac{d\tau}{\tau} = 1 \tag{3}$$

where t_0 is the start of end-gas compression, t_i the time of auto-ignition and t the induction time, defined above. This model is used just for a first computational assessment of the advantages of the knock controlled variable compression ratio operation. The model represents major factor affecting knock. At high compression ratios, even before spark ignition, the fuel–air mixture may be compressed to a high pressure and temperature which promotes auto ignition. At low engine speeds the flame velocity is slow and thus the burn time is long, and this results in more time for auto ignition. At high engine speeds, there is less heat loss so the unburned gas temperature is higher which again promotes auto ignition. All these competing effects are included in the Douaud and Eyzat induction time correlation [35] despite their description is quite simplified.

Modeling of turbo charged engines is not a novelty [33] and the baseline turbo charged GDI engine was modeled as usual introducing the measured maps of turbine and compressor, the one of turbine given as reduced speed, reduced mass flow rate, pressure ratio and efficiency, and the one of the compressor given as actual speed and mass flow rate, pressure ratio and efficiency. The waste gate opening was adjusted to achieve stable operation within the mapped area and the measured pressure out of the compressor of the baseline turbo charged GDI engine. With alternative crank trains, the same turbocharger was used and the waste gate opening was adjusted to get the maximum boost pressure compatible with stable operation within the mapped area. The optimization of boost pressure and compression ratio for maximizing the brake fuel conversion efficiency and the brake torque output within the knock limits has not been performed at this stage because the model of the FMEP with the alternative crank train mechanisms need first to be improved to make this latter optimization meaningful. The scope of the paper is to perform a first assessment of the performance increases of the novel crank train mechanisms and not to compute the optimum compression ratio, direct injector injection profile, spark advance and waste gate opening of the turbocharger coupled to the modified crank trains.

The compression ratio was selected to be the largest possible within the limits of about the same knock resistance of the baseline GDI turbocharged engine in the worst (for knock) operating point. The CR = 15.5 value of the maximum compression ratio has been selected conservatively, and the largest values may possibly follow further refinements of the model. However, the relative benefits in terms of efficiency and torque output reduce further increasing the compression ratio, and it may not be reasonable for structural reasons to further boost the compression ratio. For what concerns the Atkinson effect, the selection of the stroke ratio is even more arbitrary than the selection of the maximum compression

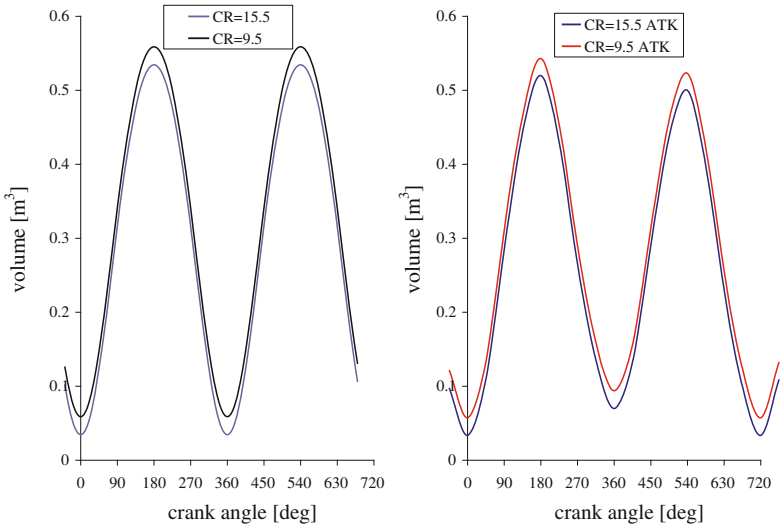

Fig. 2 Volume versus crank angle with different compression ratios without (*left*) and with (*right*) Atkinson effect

ratio described above, and a further optimized stroke ratio may follow a better consideration of the compelling efficiency benefits and structural downfalls making the mechanism more complicated.

Every user of GT-POWER knows that comparing engine concepts differing in the crank train mechanism only may start the activity from a validated engine model and then change only the minimum necessary in the model to avoid biasing the results. The proposed approach has no downfall, with the only exception of the prediction of FMEP. In the knowledge of the Authors, there is no tool able to accurately predict the FMEP of a novel innovative crank train mechanism as the one proposed. Unfortunately the use of the Chen–Flynn correlation [33] with the same parameters of the baseline engine with a standard crank train is the only option to produce an estimation of the FMEP the new mechanisms could have before testing on an engine dynamometer a prototype of an engine with the novel mechanism.

Figure 2 presents the in-cylinder volume over the 4 strokes of the engine for a power stroke. The combustion Top Dead Centre (TDC) is located at 0° crank angle. Figure 2 on left refers to the operation with variable ratio of minimum to maximum volumes but no Atkinson cycle effect, while Fig. 2 on right refers to the operation with the Atkinson cycle effect enabled.

Figure 3 presents the brake mean effective pressure (BMEP), brake efficiency and power for operation full load with the 9.5 compression ratio determined by the necessity to avoid knock around 3,000 Rpm, and for operation with a variable compression ratio higher than that for a similar margin to knock over the full range of engine speeds. The adoption of compression ratios larger than 9.5 improves the

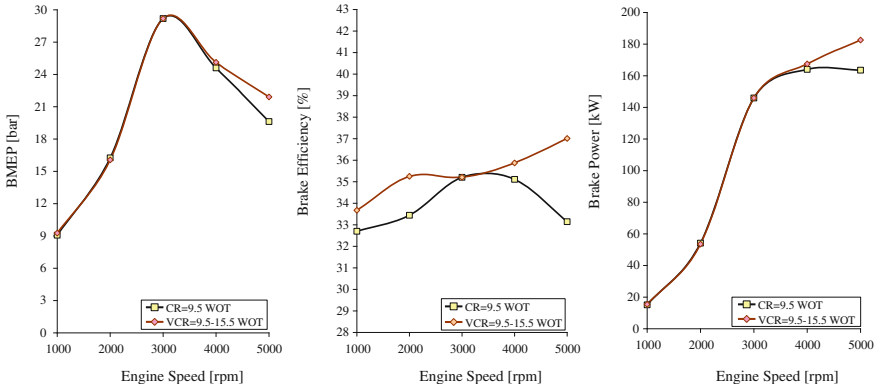

Fig. 3 BMEP, brake thermal efficiency and power with fixed and variable (maximum efficiency limited by knock) compression ratio

fuel conversion efficiency as well as the power and torque outputs especially at the higher speeds. Operating at full load with variable CR, a CR = 9.5 is used at 3,000 rpm, while higher CR are then used above and below this engine speed. At 5,000 rpm, the maximum CR = 15.5 is used, while lower values are adopted at low engine speeds. The 1,000 rpm is more critical for knock than the 2,000 rpm and the knock likeliness for the 4,000 rpm is in between the 3,000 and the 5,000 rpm points.

Figure 4 presents the part load efficiencies operating respectively at 20, 15, 10, 5, 2.5 and 1 bar BMEP with the fixed compression ratio 9.5 and no Atkinson, with a variable compression ratio 9.5–15.5 to maximize efficiency while keeping same safety to knock and no Atkinson, and finally with the variable compression ratio 9.5–15.5 and the Atkinson effect. Operating at part load with variable CR, as a general trend the operating CR is increased when reducing the load, even if some exception occurs especially at higher loads, where a lower CR may occasionally be required to provide same propensity to knock than in a point at higher load and same speed. At 1 bar and 2 bar BMEP load, obviously CR = 15.5 at all the speeds. At full load, the Atkinson effect produces a significant reduction in torque and power outputs. However, starting from high loads there are some points of operation where the engine benefits in terms of fuel conversion efficiency from adoption of the Atkinson effect. The benefits of the variable compression ratio are already evident at high loads. Reducing the loads, the benefits of the variable compression ratio are still significant and the Atkinson effect further improves the fuel conversion efficiency. At 7.5 bar BMEP, the fuel conversion efficiency improves by up to 30 % thanks to the coupled effect of variable compression ratio and Atkinson. At 5 and 2.5 bar BMEP the coupled effect of variable compression ratio and Atkinson almost double the fuel conversion efficiency. At 1 bar BMEP, the fuel conversion efficiency improvements reduce but are still around 30–50 % better.

Due to the use of a same coefficient Chen–Flynn correlation, differences in FMEP are minimal (only the different maximum pressure may introduce

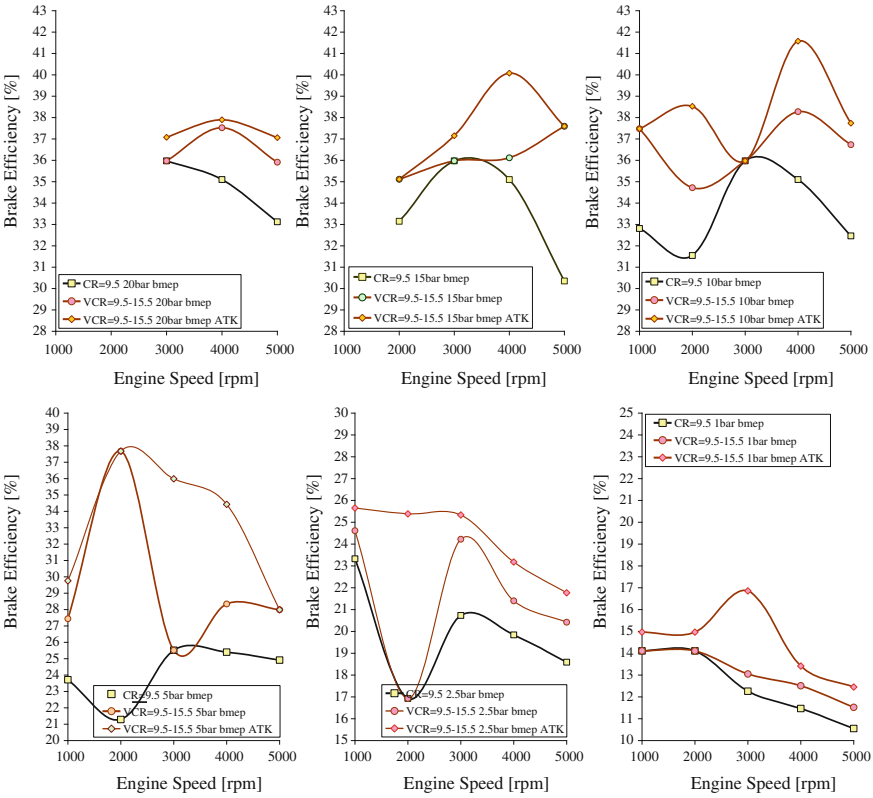

Fig. 4 Brake thermal engine efficiency with fixed compression ratio, variable compression ratio (maximum efficiency limited by knock) and variable compression ratio and Atkinson effect for operation at various BMEP

differences). Changes of pumping mean effective pressure PMEP are certainly much larger but still not the driving force for brake fuel conversion efficiencies and torque outputs. The use of the proposed novel crank train mechanism is not expected to impact too much on the vehicle fuel economy through downsizing, because the increases in FMEP currently neglected what may be significant especially at higher speeds it may offset the increase in IMEP producing the increase in top power output.

4 Kinetic Energy Recovery System

Fuel economy is measured over test cycles. The ECE + EUDC cycle is a test cycle performed on a chassis dynamometer used for emission certification of light duty vehicles in Europe [EEC Directive 90/C81/01]. The entire cycle includes four

Table 3 Main characteristics of ECE and EUDC cycles

Characteristics	ECE 15	EUDC
Distance (km)	$4 \times 1.013 = 4.052$	6.955
Duration (s)	$4 \times 195 = 780$	400
Average speed (km/h)	18.7 (with idling)	62.6
Maximum speed (km/h)	50	120

ECE segments, repeated without interruption, followed by one EUDC segment. Before the test, the vehicle is allowed to soak for at least 6 h at a test temperature of 20–30 °C. It is then started and the emission sampling begins at the same time. This cold-start procedure is also referred to as the New European Driving Cycle (NEDC). The ECE cycle is an urban driving cycle, also known as UDC. It was devised to represent city driving conditions, e.g. in Paris or Rome. It is characterized by low vehicle speed, low engine load, and low exhaust gas temperature. The EUDC (Extra Urban Driving Cycle) segment has been added after the fourth ECE cycle to account for more aggressive, high speed driving modes. The maximum speed of the EUDC cycle is 120 km/h. Table 3 summarizes the parameters for both the ECE and EUDC cycles.

Being cycles characterized by accelerations following decelerations, the energy needed to re accelerated a car following a deceleration may be reduced recovering the braking energy. This is done more efficiently with mechanical rather than electric systems. It is a fundamental of physics that transforming energy from one form to another inevitably introduces significant losses. This explains why the efficiency of battery-based hybrids is so low for a regenerative braking cycle. When a battery is involved, there are four efficiency reducing transformations in each regenerative braking cycle. (1) Kinetic energy is transformed into electrical energy in a motor/generator, (2) the electrical energy is transformed into chemical energy as the battery charges up, (3) the battery discharges transforming chemical into electrical energy, (4) the electrical energy passes into the motor/generator acting as a motor and is transformed once more into kinetic energy. The four energy transformations reduce the overall level of efficiency. If the motor/generator operates at 80 % efficiency under peak load, in and out, and the battery charges and discharges at 75 % efficiency at high power, the overall efficiency over a full regenerative cycle is only 36 %. The ideal solution is thus to avoid all four of the efficiency reducing transformations from one form of energy to another by keeping the vehicle's energy in the same form as when the vehicle starts braking when the vehicle is back up to speed. This can be done using high-speed flywheels [26–32]. A mechanically driven flywheel system has losses, due to friction in bearings and windage effects, which make it less efficient than a battery-based system in storing energy for long times. Over the much shorter periods required in cut-and-thrust traffic, a mechanically driven flywheel is much more effective, providing an overall efficiency over a full regenerative cycle of more than 70 %, almost twice the value of battery-based hybrids [26–32] (Fig. 5).

Figure 6 presents the prescribed velocity, acceleration, product of velocity by acceleration and kinetic energy of a passenger car covering the NEDC. The

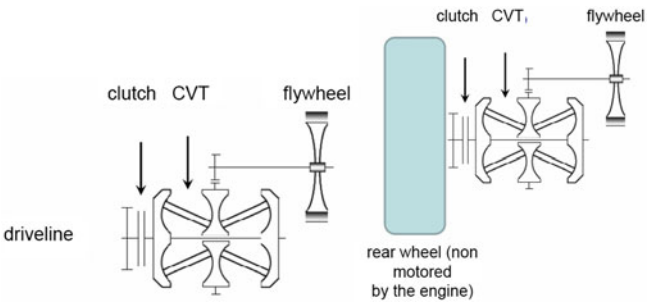

Fig. 5 Schematic flywheel of the driveline (*left*) and a non driveline (*right*) mechanical hybrid systems

acceleration is roughly the propulsive or the braking force per unit mass of the car, while the product of velocity by acceleration is roughly the propulsive or the braking power per unit mass of the car and the kinetic energy difference over a braking event is roughly the theoretically available braking energy. Neglecting the unrealistic final deceleration where the car comes to rest from 120 km/h in few seconds that no European driver has possibly never covered and all the braking energy with a mechanical KERS is lost, a passenger car KERS can be designed to store less energy and with a smaller charging or discharging rate and over a reduced time than a 60 kW–0.4 MJ 2009 F1 strategic KERS or a 120 kW–2 MJ 2014 F1 strategic and fuel economy KERS. The braking power is less than 7.5 W per kg of mass of the car over the city driving sections. This translates in braking powers of only 9 kW for a 1,200 kg car. The braking energy is less than 100 J per kg of mass of the car over the city driving sections. This translates in braking energy to be stored of only 120 kJ for a 1,200 kg car. These and not the F1 figures are the numbers that passenger car KERS must be designed for.

While the first generation KERS for passenger car applications was derived from the 2009 F1 KERS design [36, 37], the second generation KERS is being developed for much smaller braking powers and braking energy than those of 2009/2011 and 2014 F1 KERS. Furthermore, the braking energy is used immediately after stored, and this further facilitates the design. Also focusing on the CVT that is the most inefficient part of the KERS and the off driveline configuration working on the non motored wheels, the latest designs have shown the opportunity to increase the round trip efficiency wheels-flywheels-wheels of a regenerative braking event from the 70 % of the first generation to the 80 % of this second generation while achieving a cost for mass production estimated in the order of 600 $.

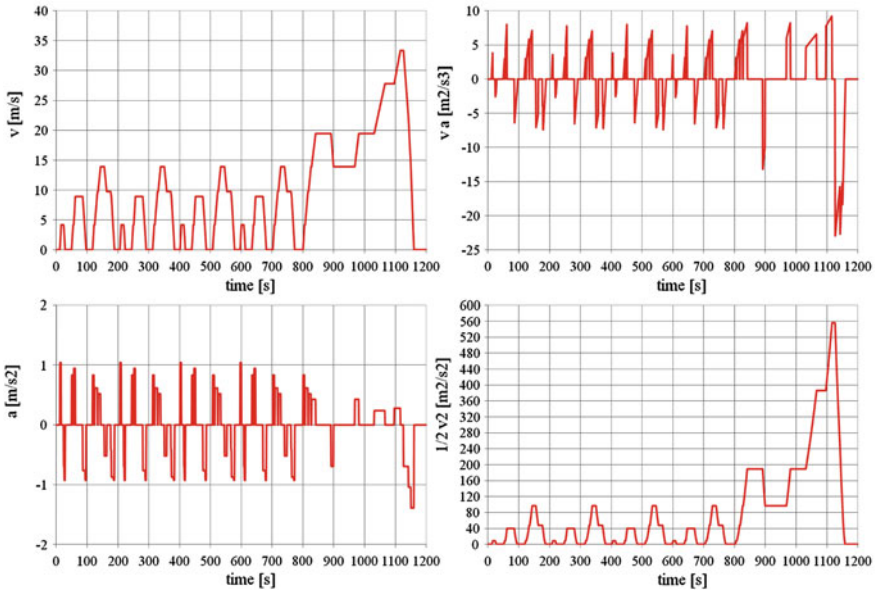

Fig. 6 Prescribed velocity, acceleration, product of velocity by acceleration and kinetic energy of a passenger car covering the NEDC

5 Vehicle Fuel Economy Results

New European Driving Cycle (NEDC) simulations have then been performed with the Lotus Vehicle Simulation software [38]. In order to calculate the vehicle environmental friendliness, we use here the fuel energy in addition to the CO_2 emission as a parameter, and we use two conventional hydrocarbon fuels to replace pump Diesel and Gasoline/Petrol. We use here the GT-SUITE reference fuels "*Diesel no. 2"* for Diesel, and "*Indolene*" for Gasoline/Petrol [33]. For this conventional Diesel fuel, C = 13.5, H = 23.6 and LHV = 43,250 kJ/Kg, while for the conventional Gasoline/Petrol fuel C = 7.93, H = 14.8 and LHV = 43,950 kJ/Kg. Generally, the chemical equation for stoichiometric burning of hydrocarbon in oxygen is:

$$C_nH_m + (n + \frac{m}{4}) \cdot O_2 \rightarrow n \cdot CO_2 + \frac{m}{2} \cdot H_2O \tag{4}$$

and CO_2 emissions can be computed accordingly. Average CO_2 emissions from these hydrocarbon fuels are computed considering an oxidation factor to be applied to the carbon content to account for a small portion of the fuel that is not oxidized into CO_2. The IPCC [39] guidelines for calculating emissions inventories require that for all oil and oil products, the oxidation factor is 0.99 (99 % of the carbon in the fuel is eventually oxidized, while 1 % remains un-oxidized). Therefore we assume a production of CO_2 of 2621 and 2332 g/L for Diesel and Gasoline/Petrol fuels respectively.

Table 4 Full size passenger car vehicle parameters

Mass m (kg)	1810
Frontal area A (m^2)	2.250
Drag coefficient C_D	0.298
Rolling tire radius R (m)	0.3160
Transmission	5-speed automatic
Transmission ratios	3.22/2.29/1.55/1.00/0.75
Final drive ratio	2.730

The novel crank train mechanism is obviously expected to produce much larger benefits during the city driving rather than the highway driving, but this obviously depends on the actual engine BMEP and speed operating points covered during the cycle and where they fall in the BSFC versus BMEP and speed map of the engine, ultimately a function of vehicle mass and aerodynamic as well as of gear and final drive ratios just to name the most influencing parameters.

5.1 Full Size Passenger Car

NEDC simulations have been performed first for a large full size passenger car equipped with a 4 litres naturally aspirated gasoline engine and with the new 2 L turbo GDI engine described above. The main vehicle parameters are summarized in Table 4. The model has been validated for the car equipped with the 4 litres naturally aspirated, port fuel injection gasoline engine, with computed fuel economies within a 5 % of measured values. The cold start behaviour is simulated. The vehicle model is then modified to use the brake specific fuel consumption maps of the 2 litres high power density, turbo charged, direct injection, gasoline engines with fixed compression ratio 9.5, variable compression ratio 9.5–15.5, and finally variable compression ratio 9.5–15.5 and Atkinson cycle effects. These changes that could be extremely costly on a real vehicle just require a few modification of the model to obtain fuel economies that are expected not to be that far from actual values. Figure 7 presents the brake specific fuel consumption maps for the 4 litres naturally aspirated gasoline engine and the 2 L GDI turbo charged engines with fixed compression ratio, variable compression ratio and variable compression ratio plus variable stroke ratio.

The 4 L, in-line six cylinders, throttle body controlled, naturally aspirated gasoline engine with maximum power 190 kW and maximum torque 380 N m is replaced by the high tech, 2L, in-line four, turbo charged gasoline engines described above, having 164.0 kW maximum power and 464.5 N m maximum torque with compression ratio 9.5 and 182.6 kW maximum power and 464.5 N m maximum torque with variable compression ratio 9.5–15.5 (the Atkinson effect is active at low loads only). Downsizing permits reduced top speeds but sharpest accelerations with reference to the baseline large gasoline engine. Vehicle, tyre,

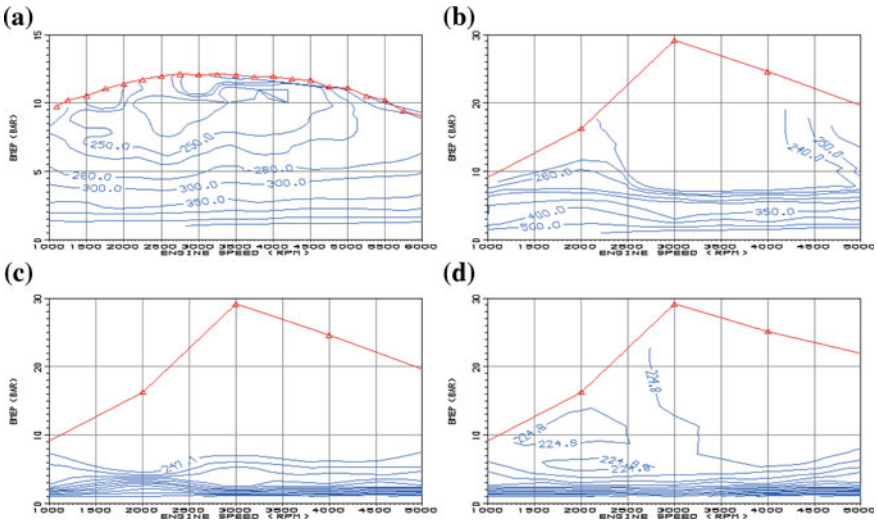

Fig. 7 Brake specific fuel consumption maps for the **a** 4 L naturally aspirated gasoline engine, **b** 2 L GDI turbo charged engines with fixed compression ratio (FCR), **c** 2 L GDI turbo charged variable compression ratio (VCR), **d** 2 L GDI turbo charged VCR and variable stroke ratio (ATK)

driveline and gearbox data are kept constant, as well as the shift strategy, that is the one defined for optimum use of the 4L gasoline engine. During braking the fuel flow rate is the zero BMEP value for the selected speed. The displacement effect shifts up by a factor of 4/2 = 2 the operating BMEP versus engine speed of the small engines. The naturally aspirated 4L gasoline engine works the most of the time at 1.5 bar BMEP and 1500 rpm, while the turbocharged 2L gasoline engines work the most of the time at 3 bar BMEP and 1500 rpm. Table 5 summarizes the fuel economy results of the different engines.

Despite the shift strategy and that the gear ratios are not optimized for the 2 L engine, all the three high power density TC GDI engines produce dramatic improvements in the fuel usage over the cycle. While the 4 L gasoline engine uses 937 g of fuel to cover over the 1180 s total cycle time the 11.028 km distance travelled of the NEDC for a fuel consumption of 11.3 L per 100 km, the downsized 2 L TC GDI CR = 9.5 engine already provides a 29 % better fuel economy, with 738 g of fuel used in the test or a fuel consumption of 8.9 L per 100 km. The adoption of the variable compression ratio VCR = 9.5–15.5 in the 2 L TC GDI engine boost the fuel economy of an additional 12.7 %, while the further adoption of the Atkinson effect expands of another 5.7 % the fuel economy benefits.

In terms of fuel energy, the small high tech engine 2 L TC GDI VCR = 9.5–15.5 with Atkinson effect therefore uses 53 % less fuel energy than the large naturally aspirated low tech gasoline engine. This is due to the higher BMEP permitted by downsizing (two times larger operating BMEP following the displacement ratio), the larger top brake efficiency permitted by the high compression ratio, the cooling due to

Table 5 Fuel consumption results for the full size passenger car equipped with the 4 L naturally aspirated gasoline and the 2 L Turbo GDI engines with various crank trains

Engine	4 L NA Gasoline	2 L TC GDI CR = 9.5 engine	2 L TC GDI VCR = 9.5–15.5	2 L TC GDI VCR = 9.5–15.5 Atkinson effect
Power train	std	std	std	std
Litres per 100 km	11.33	8.79	7.80	7.38
km per litre	8.83	11.38	12.82	13.55
Grams per km	84.94	65.91	58.50	55.34
MJ of fuel energy per km	3.73	2.90	2.57	2.43
Fuel efficiency improvement (%)	0.00	22.40	31.12	34.85
		0.00	11.24	16.05
			0.00	5.41
Grams of CO_2 per km	264.2	205.0	181.9	172.1
CO_2 emission improvement (%)	0.00	22.40	31.12	34.85
		0.00	11.24	16.05
			0.00	5.41

Table 6 Compact size passenger car vehicle parameters

Mass m (kg)	1336
Frontal area A (m^2)	2.2
Drag coefficient C_D	0.298
Rolling tire radius R (m)	0.3080
Transmission	5-speed manual
Transmission ratios	3.778/1.944/1.185/0.816/0.625
Final drive ratio	3.389

direct injection, the high boost from turbo charging partially recovering the exhaust waste heat, the spark advances closer to maximum brake torque, and the larger part load efficiencies due to the factors above plus the variable compression ratio and the Atkinson effect.

5.2 Compact Size Passenger Car

NEDC simulations have then been performed for a small compact size passenger car equipped with a 1.6 L Diesel TDI engine and with a version downsized to 1 L of the new 2 L turbo GDI engine described above. For sake of simplicity, the 1 L turbo GDI engine is supposed to be obtained by scaling all the geometrical parameters to produce (about) the same indicated specific fuel consumption (ISFC) curves versus IMEP and speed but a curve of friction mean effective pressure (FMEP) versus speed improved for the lower mean piston speed (stroke of 68 mm vs. the 86 mm of the 2 L engine). Consequently, if ΔFMEP is the difference in FMEP computed with the longer and shorter stroke, a very first approximation of the BSFC curves versus BMEP and speed is obtained multiplying by the ratio IMEP/(IMEP + ΔFMEP), while a very first approximation of the curve of WOT BMEP versus speed is obtained dividing by the ratio IMEP/(IMEP + ΔFMEP). These results are obviously only preliminary.

The main vehicle parameters are summarized in Table 6. The model has been validated for the car equipped with the 1.6 L TDI Diesel engine, with computed fuel economies within a 5 % of measured values. The cold start behaviour is simulated. The vehicle model is then modified to use the brake specific fuel consumption maps of the 1 L high power density, turbo charged, direct injection, gasoline engines with fixed compression ratio 9.5, variable compression ratio 9.5–15.5, and finally variable compression ratio 9.5–15.5 and Atkinson cycle effects. These changes that could be extremely costly on a real vehicle just require a few modification of the model to obtain fuel economies that are expected not to be that far from actual values.

The 1.6 L TDI Diesel engine with maximum power 81 kW and maximum torque 250 N m is replaced by the high tech, 1 L, in-line four, turbo charged gasoline engines described above, having 82 kW maximum power and 233 N m maximum torque with compression ratio 9.5 and 91.3 kW maximum power and

Table 7 Fuel consumption results for the compact size passenger car equipped with the 1.6 TDI diesel and 0.9 L TGDI gasoline engines with first and second generation mechanical KERS

Engine	1.6 L TDI diesel	1 L TC GDI CR = 9.5 engine	1 L TC GDI VCR = 9.5–15.5	1 L TC GDI VCR = 9.5–15.5 Atkinson effect	1 L TC GDI VCR = 9.5–15.5 Atkinson effect	1 L TC GDI VCR = 9.5–15.5 Atkinson effect
Power train	std	std	std	std	KERS 1st generation	KERS 2nd generation
Round trip regenerative braking efficiency (%)	0	0	0	0	70	80
Fuel lower calorific value (kJ/kg)	43,250	43,950	43,950	43,950	43,950	43,950
Hydrocarbon fuel composition	C = 13.5 H = 23.6	C = 7.93 H = 14.8	C = 7.93 H = 14.8	C = 7.93 H = 14.8	C = 7.93 H = 14.8	C = 7.93 H = 14.8
Fuel density (kg/L)	0.835	0.75	0.75	0.75	0.75	0.75
CO_2 production (g/L)	2621	2332	2332	2332	2332	2332
Litres per 100 km	3.85	5	4.5	4.22	3.42	3.31
km per Litre	25.98	20.01	22.22	23.68	29.24	30.27
Grams per km	32.14	37.49	33.75	31.67	25.65	24.79
MJ of fuel energy per km	1.39	1.65	1.48	1.39	1.13	1.09
Fuel efficiency improvement (%)	0.00	−18.55	−6.72	−0.14	18.88	21.42
		0.00	9.98	15.52	31.57	33.80
			0.00	6.16	23.99	26.20
				0.00	19.00	21.42
g of CO_2 per km	100.9	116.6	105	98.5	79.80	77.13
CO_2 emission improvement (%)	0.00	−15.60	−4.07	2.35	20.90	23.55
		0.00	9.98	15.52	31.57	33.85
			0.00	6.16	23.99	26.54

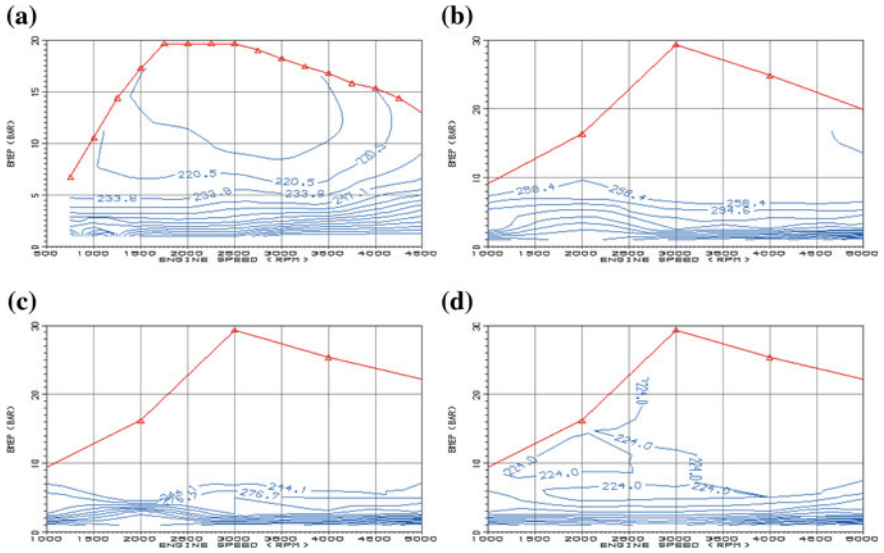

Fig. 8 Brake specific fuel consumption maps for the **a** 1.6 L TDI Diesel, **b** 1 L GDI turbo charged engines with FCR, **c** 1 L GDI turbo charged engines with VCR **d** 1 L GDI turbo charged engines with VCR and ATK

233 N m maximum torque with variable compression ratio 9.5–15.5 (the Atkinson effect is active at low loads only). Downsizing permits same top speeds and sharpest accelerations with reference to the baseline Diesel engine because of the low power density of lean burn Diesel. Vehicle, tyre, driveline and gearbox data are kept constant, as well as the shift strategy, that is the one defined for optimum use of the 1.6 TDI Diesel engine. During braking the fuel flow rate is the zero BMEP value for the selected speed. The displacement effect shifts up by a factor 1.6 the operating BMEP versus engine speed of the small engines. Table 7 summarizes the fuel economy results of the different engines.

Despite the shift strategy and the gear ratios are not optimized for the 1L engine, the high power density TC GDI engines with VCR and with and without Atkinson effect produce fuel usages over the cycle comparable to Diesel. The adoption of the variable compression ratio VCR = 9.5–15.5 and Atkinson effect in the 1 L TC GDI engine boost the fuel economy to values similar to those of best available Diesel engines. Despite the Diesel has much better top as well as part load fuel efficiencies for the lean combustion and the throttle-less load control by quantity of fuel injected, the downsizing of the higher power density gasoline engine and the part load benefits of VCR and Atkinson effect even in an engine controlled by throttle and stoichiometric produce about same fuel energy economy over the NEDC and about same CO_2 production. Figure 8 presents the brake specific fuel consumption maps for the 1.6 L TDI Diesel engine and the 1 L GDI turbo charged engines with fixed compression ratio, variable compression ratio and variable compression ratio plus variable stroke ratio.

Engine performance and vehicle fuel economy simulations are very well established approaches; with very well know abilities to well predict engine and chassis dynamometer results for engines and power train not differing too much from those used for the preliminary validation of the model. The baseline model for the engine, with turbo charging and GDI and a traditional crank train, and the baseline model for the vehicle, with the measured BSFC versus BMEP and speed of the engine above as an input and the traditional power train, are validated models. Changes in the crank train mechanism that concerns the engine and in the kinetic energy recovery system that concern the vehicle power train are not expected to reduce too much the reliability of the results, even if their modeling certainly introduces the uncertainties only of the final engine dynamometer and chassis vehicle dynamometer tests of the prototypes engine and vehicle may dissipate.

6 Conclusions

The paper has presented a new mechanism able to change the compression ratio of the engine as well as the ratio between the compression and the expansion strokes. This brings advantages over the full range of loads and speeds. Operation with the maximum compression ratio permitted by knock improves the fuel efficiency over the full range of loads and also increases the maximum power output. Addition of the Atkinson effect helps to further boost the medium to low load efficiency.

Simulations performed for a 2 L turbocharged GDI engine show that adjusting the compression ratio from the low speed knock limited value of CR = 9.5:1 to achieve about same margin to knock all over the range of engine speeds and loads up to a CR of 15:1, the maximum power is increased by 11 % and the maximum brake efficiency by 3.3 %, while operating at 1 bar BMEP and 2 bar BMEP fuel conversion efficiencies are up to 10 % better. The benefits of the variable compression ratio increase reducing the loads. The Atkinson effect further improves the fuel conversion efficiency especially at very low loads.

At 7.5 bar BMEP, the fuel conversion efficiency improves of up to 30 % thanks to the coupled effect of variable compression ratio and Atkinson. At 5 and 2.5 bar BMEP the coupled effect of variable compression ratio and Atkinson almost double the fuel conversion efficiency. At 1 bar BMEP, the fuel conversion efficiency improvements reduce but are still around 30–50 % better.

Replacing a 4 L naturally aspirated gasoline engine of a full size car with the 2 L TC GDI engines produce dramatic improvements in the fuel usage over the NEDC cycle. While the 4 L gasoline engine has a fuel consumption of 11.3 Litres per 100 km, the downsized 2 L TC GDI CR = 9.5 engine provides a 29 % better fuel economy, with a fuel consumption of 8.9 L per 100 km. The adoption of the variable compression ratio VCR = 9.5–15.5 in the 2 L TC GDI engine boost the fuel economy of an additional 12.7 %, while the further adoption of the Atkinson effect provides another 5.7 % to the fuel economy benefits.

Replacing a 1.6L TDI Diesel engine of a compact size car with the 1L TC GDI engines produce about same fuel energy usage and CO_2 production with variable compression ratio VCR = 9.5–15.5 and the Atkinson effect, with a fuel economy of 4.2 L of gasoline fuel and less than 100 g of CO_2 per km.

Further improvements of the engine fuel conversion efficiency is achieved by the adoption of fully variable valve actuation (VVA) and exhaust gas recirculation (EGR) to control the load throttle less thus reducing the pumping losses as well as to improve the efficiency of the combustion process changing speed and load [40, 41].

Significant improvements of the vehicle fuel economy may be further enhanced by the adoption of a purely mechanical flywheel based Kinetic Energy Recovery System (KERS) [36, 37] dramatically reducing the amount of energy to be delivered by the thermal engine. The 1 L TC GDI engine with variable compression ratio and Atkinson effect installed on a compact car may permits when coupled to a first generation kinetic energy recovery system a fuel economy of 1.13 MJ of fuel energy per km and tailpipe CO_2 emissions of 79.8 g of CO_2 per km.

The fuel economy and the tailpipe CO_2 emissions may be further reduced to 1.09 MJ of fuel energy per km and 77.1 g of CO_2 per km by moving to second generation KERS specifically developed for the low power and low energy storage and short times of the passenger car applications, where also focusing on the CVT and using non driveline configurations the round trip efficiencies of the regenerative braking process are currently projected to the 80 % mark from the previous 70 %.

In terms of CO_2 reduction, an evolutionary breakthrough may be the eventual replacement of fossil fuels like gasoline with bio fuels like ethanol being almost carbon neutral in the short term rather than over geological ages. The bio ethanol also has the advantage of the increased resistance to knock especially in a direct injection engine, thanks to the better octane number as well as the larger heat of vaporization, translating in higher compression ratios, spark timings closer to maximum brake torque and higher boost pressures than gasoline, for better fuel conversion efficiencies and power density the latter permitting further downsizing [40, 41].

References

1. EPA report (2010) A study of potential effectiveness of carbon dioxide reducing vehicle. technologies. http://www.epa.gov/oms/technology/420r08004a.pdf. Retrieved 1 Sept 2010
2. EERE report (2010) 2009 Advanced combustion engine R&D annual report. http://www1.eere.energy.gov/vehiclesandfuels/pdfs/program/2009_adv_combustion_engine.pdf. Retrieved 1 Sept 2010
3. Saunders RJ et al (1989) Variable valve closure timing for load control and the Otto Atkinson cycle engine. SAE paper 890677
4. Blakey SC et al (1991) A design and experimental study of an Otto Atkinson cycle engine using late intake valve closing. SAE paper 910451
5. Boggs DL et al (1995) The Otto–Atkinson cycle engine-fuel economy and emissions results and hardware design. SAE paper 950089

6. CaoY (2007) Thermodynamic cycles of internal combustion engines for increased thermal efficiency, constant-volume combustion, variable compression ratio, and cold start. SAE paper 2007-01-4115
7. Gheorghiu V (2009) CO_2-emission reduction by means of enhanced thermal conversion efficiency of ice cycles. SAE paper 2009-24-0081
8. Gheorghiu V (2010) CO_2-emission reduction by means of enhancing the thermal conversion efficiency of ice cycles. SAE paper 2010-01-1511
9. Shkolnik N et al (2010) High efficiency hybrid cycle engine. SAE paper 2010-01-1110
10. Akihisa D et al (2010) Research on improving thermal efficiency through variable super-high expansion ratio cycle. SAE paper 2010-01-0174
11. Wallace WA, Lux FB (1964) A variable compression ratio engine development. SAE paper 640060
12. Basiletti JC, Blackburne EF (1966) Recent developments in variable compression ratio engines. SAE paper 660344
13. Sobotowski R et al (1991) The development of a novel variable compression ratio, direct injection diesel engine. SAE paper 910484
14. Pischinger S et al (2001) Variable compression in SI engines. SAE paper 2001-24-0050
15. Mendler C, Gravel R (2002) Variable compression ratio engine. SAE paper 2002-01-1940
16. Schwaderlapp M et al (2002) Variable compression ratio—a design solution for fuel economy concepts. SAE paper 2002-01-1103
17. Moteki K et al (2003) A study of a variable compression ratio system with a multi-link mechanism. SAE paper 2003-01-0921
18. Roberts M (2003) Benefits and challenges of variable compression ratio (VCR). SAE paper 2003-01-0398. http://www.prodrive.com/up/vcr.pdf. Retrieved 2 Aug 2010
19. Rabhi V, Beroff J (2004) Study of a gear-based variable compression ratio engine. SAE paper 2004-01-2931
20. Rabhi D et al (2005) Gear design and dimensioning study for a variable compression ratio engine. SAE paper 2005-01-3131
21. Rosso P et al (2006) A variable displacement engine with independently controllable stroke length and compression ratio. SAE paper 2006-01-0741
22. Tanaka Y et al (2007) A study of a compression ratio control mechanism for a multiple-link variable compression ratio engine. SAE paper 2007-01-3547
23. Ishikawa S et al (2009) Advanced design of variable compression ratio engine with dual piston mechanism. SAE paper 2009-01-1046
24. Kadota M et al (2009) advanced control system of variable compression ratio (VCR) engine with dual piston mechanism. SAE paper 2009-01-1063
25. Heywood JB (2005) Improving the spark-ignition engine. In: 2005 ERC symposium, Madison, WI (US), June 2005. http://www.erc.wisc.edu/documents/symp05-Heywood.pdf. Retrieved 2 Aug 2010
26. Stone R (2009) Full-toroidal variable drive transmission systems in mechanical hybrid systems—from Formula 1 to road cars. In: CTI symposium and exhibition: automotive transmissions, Berlin, Germany, December 2009. http://www.torotrak.com/Resources/Torotrak/Documents/Mech%20hybrid%20paper_CTI%20Berlin09.pdf. Retrieved 11 November 2011)
27. Body W, Brockbank C (2009) Simulation of the fuel consumption benefits of various transmission arrangements and control strategies within a flywheel based mechanical hybrid system. In: VDI transmissions in vehicles conference and exhibition, Friedrichshafen, June 2009. http://www.torotrak.com/Resources/Torotrak/Documents/VDI%20Friedrichshafen%202009.pdf. Retrieved 11 November 2011)
28. Brockbank C, Greenwood C (2009) Full-toroidal variable drive transmission systems in mechanical hybrid systems—from Formula 1 to road vehicles. In: CTI symposium and exhibition: automotive transmissions, Detroit, May 2009. http://www.torotrak.com/Resources/Torotrak/Documents/CTI%20Detroit%20Paper%202009.pdf. Retrieved 11 November 2011)

29. Brockbank C (2009) Application of a variable drive to supercharger and turbo compunder applications. SAE paper. 09PFL-0925. http://www.torotrak.com/Resources/Torotrak/Documents/SAE_WC_2009_09PFL-0925_Variable_Drive_Boost_System.pdf. Retrieved 11 November 2011)
30. Brockbank C, Cross D (2009) Mechanical hybrid system comprising a flywheel and CVT for motorsport and mainstream automotive applications. SAE paper 09PFL-0922. http://www.torotrak.com/Resources/Torotrak/Documents/SAE_WC_2009_09PFL-0922_KERS.pdf. Retrieved 11 Nov 2011)
31. Brockbank C, Greenwood C (2008) Full-toroidal variable drive transmssion systems in mechanical hybrids—from Formula 1 to road vehicles. In: CTI innovative automotive transmissions conference and exhibition, Berlin, December 2008. http://www.torotrak.com/Resources/Torotrak/CTI_Berlin_2008.pdf. Retrieved 11 Nov, 2011
32. Brockbank C, Greenwood C (2008) Formula 1 mechanical hybrid applied to mainstream automotive. In: VDI Getriebe in Fahrzeuge Conference, June 2008. http://www.torotrak.com/Resources/Torotrak/VDI_2008.pdf. Retrieved 11 Nov 2011
33. http://www.gtisoft.com/products/p_GT_SUITE.php. Retrieved 1 Sept 2010
34. Chen SK, Flynn PF (1965) Development of single cylinder compression ignition research engine. SAE paper 650733
35. Douaud AM, Eyzat P (1978) Four-octane-number method for predicting the anti-knock behavior of fuels and engines. SAE paper 780080
36. Boretti A (2010) Comparison of fuel economies of high efficiency diesel and hydrogen engines powering a compact car with a flywheel based kinetic energy recovery systems. Int J Hydrogen Energy. doi:/10.1016/j.ijhydene.2010.05.031
37. Boretti A (2010) Improvements of vehicle fuel economy using mechanical regenerative braking. In: SAE paper 2010-01-1683 at SAE 2010 annual brake colloquium and engineering display, Phoenix, AZ, USA, October 2010
38. http://www.lesoft.co.uk/index1.html. Retrieved 20 Jan 2010
39. http://www.ipcc.ch/. Retrieved 13 Sept 2010
40. Boretti A (2010) Performances of a turbocharged E100 engine with direct injection and variable valve actuation. In: SAE paper 2010-01-2154 at SAE 2010 power trains, fuels and lubricants meeting, San Diego, CA, USA, October 2010
41. Boretti A (2010) Use of variable valve actuation to control the load in a direct injection, turbocharged, spark-ignition engine. In: SAE paper 2010-01-2225 at SAE 2010 power trains, fuels and lubricants meeting, San Diego, CA, USA, October 2010
42. http://www.direct.gov.uk/en/Motoring/OwningAVehicle/HowToTaxYourVehicle/DG_4022118. Retrieved 13 Sept 2010
43. http://www.vcacarfueldata.org.uk/. Retrieved 13 Sept 2010
44. http://carboncalculator.direct.gov.uk/index.html. Retrieved 13 Sept 2010